# Supplementary Materials for

# Molecular Dynamic simulation study on Hydrocarbon ladder polymer membranes for gas separation

**Wenxuan Tian,[a] Lidong Gong,[*a] Chunyang Yu,[*bc], Yongfeng Zhou[bc]**

[a.] *School of Chemistry & Chemical Engineering, Liaoning Normal University, 850 Huanghe Road, Dalian, China 116029*

[b.] *School of Chemistry & Chemical Engineering, Frontiers Science Center for Transformative Molecules, Shanghai Key Laboratory of Electrical Insulation and Thermal Aging, Shanghai Jiao Tong University, 800 Dongchuan Road, Shanghai, China 200240*

[c.] *Key Laboratory of Green and High-end Utilization of Salt Lake Resources, Chinese Academy of Sciences*

*E-mail: gongjw@lnnu.edu.cn; chunyangyu@sjtu.edu.cn*

# S-1.1 Force field parameterization

In this simulation, the TraPPE force field was employed for gas molecules. Two virtual sites were assigned to $CO_2$ for mass distribution, while one virtual site was introduced for $N_2$ to distribute its charge. Detailed parameters are listed in Table S1. For Me2F and DHP, parameters were obtained from the GAFF force field, as outlined in Tables S2 and S3.

**Table S1.** Atomic parameters of TraPPE Force field for gas molecules.

| Atom type | ε (KJ/mol) | σ (nm) | mass | Force Field |
|---|---|---|---|---|
| O_$CO_2$ | 0.31 | 0.66 | 0.00 | TraPPE |
| C_$CO_2$ | 0.28 | 0.22 | 0.00 | TraPPE |
| M_$CO_2$ | 0.00 | 0.00 | 22.00 | TraPPE |
| N_$N_2$ | 0.33 | 0.30 | 14.00 | TraPPE |
| N_com | - | - | 0.00 | TraPPE |

**Table S2.** Atomic parameters of GAFF Force field for DHP repeat unit.

| Atom type | ε (KJ/mol) | σ (nm) | mass | Force Field |
|---|---|---|---|---|
| ca | 0.36 | 0.34 | 12.01 | GAFF |
| c3 | 0.46 | 0.34 | 12.01 | GAFF |
| hc | 0.07 | 0.26 | 1.00 | GAFF |
| cy | 0.36 | 0.34 | 12.01 | GAFF |
| ha | 0.06 | 0.26 | 1.00 | GAFF |
| cx | 0.36 | 0.34 | 12.01 | GAFF |

**Table S3.** Atomic parameters of GAFF Force field for Me2F repeat unit.

| Atom type | ε (KJ/mol) | σ (nm) | charge | mass | Force Field |
|---|---|---|---|---|---|
| cy | 0.36 | 0.34 | 0.12 | 12.01 | GAFF |
| c3 | 0.46 | 0.34 | 0.70 | 12.01 | GAFF |
| hc | 0.07 | 0.26 | 0.00 | 1.00 | GAFF |
| ca | 0.36 | 0.34 | -0.48 | 12.01 | GAFF |
| ha | 0.06 | 0.26 | | 1.00 | GAFF |
| cp | 0.36 | 0.34 | | 12.01 | GAFF |
| cx | 0.46 | 0.34 | | 12.01 | GAFF |
| co | 0.46 | 0.34 | 0.96 | 12.01 | GAFF |

## S-1.2 Initial structure characterization

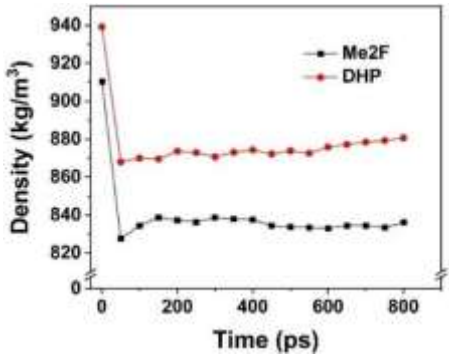


**Figure S1.** Density of the Me2F and DHP membranes after 21 steps compression.

To reflect real target density, a 21-step annealing compression process was applied to Me2F and DHP membranes. The densities of both membranes stabilized over the final 800 ps, indicating the system reached an equilibrium state, as shown in Figure S1.

After achieving a stable structure, detailed characterization and visualization of the polymer membranes were performed using Zeo++. Zeo++ calculates the geometrical parameters describing pores and BET surface area. The tool is based on the Voronoi decomposition, which for a given

arrangement of atoms in a periodic domain provides a graph representation of the void space. The resulting Voronoi network is analyzed to obtain the diameter of the largest included sphere and the largest free sphere, which are two geometrical parameters that are frequently used to describe pore geometry. Accessibility of nodes in the network is also determined for a given guest molecule and the resulting information is later used to retrieve dimensionality of channel systems as well as in Monte Carlo sampling of accessible surfaces, volumes, pore size distribution histograms as well as other representations such as stochastic ray-trace histograms. The identified guest-inaccessible regions can be also characterized and the corresponding blocking spheres can be generated to facilitate molecular simulations[1].

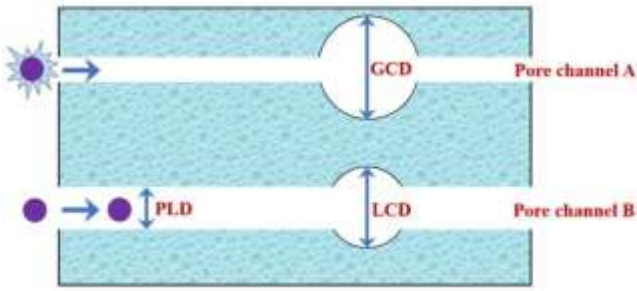


**Figure S2.** Visual illustration of GCD, PLD and LCD.

The pore of GCD, PLD and LCD as shown in Figure S2. The A-channel space in Figure S2 is inaccessible to gas molecules, although GCD might be larger than LCD. But PLD is the decisive factor for gas molecules to enter the polce cavity, and some cavities may act as dead ends and become inaccessible. In the calculation of pore diameters, GCD and LCD are not necessarily equal. The PLD more closely resembles the diameter of a channel, which is the limit diameter through which gas molecules are allowed to pass. If the diameter of gas molecules is greater than PLD, we consider the cavity to be inaccessible, whereas GCD and LCD resemble the diameters of the cavity. GCD represents the largest cavity diameter of all the channels in the entire system and LCD represents the largest cavity diameter of all the cavities in a single channel. Generally speaking, GCD is equal or greater than LCD. Except for PLD, all other indicators show that the pore size of Me2F is slightly larger than that of DHP, which may account for the superior permeability of Me2F. By combining density and pore size data, the superior permeability performance of Me2F membranes can be reasonably explained.

## S-1.3 Determination of simulation time.

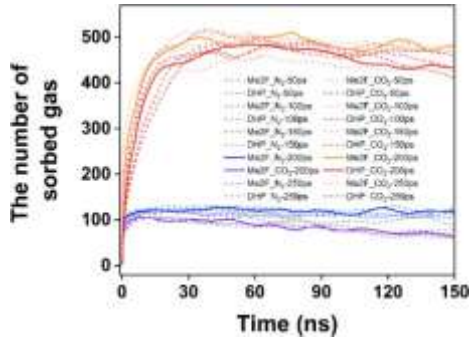


**Figure S3.** The number of gas molecules adsorbed by the membrane under different τ（τ=50ps, 100ps, 150ps, 200ps, 250ps.）

To better evaluate the simulation results and accurately reflect real conditions, the simulation box was divided into three zones: packing zone, dissolution and permeation zone, and separation zone. The total simulation time was further segmented into several smaller intervals, each with a duration of τ.

Different τ values were defined to analyse $CO_2$ and $N_2$ adsorption on membranes, as shown in Figure S3. Five τ intervals were tested to

monitor temporal variations in gas adsorption. Stability was assessed using relative deviation (absolute deviation/mean adsorption), which remained below 8% across all intervals, indicating minimal fluctuations and stable error margins. Preliminary tests validated that 200 ps ensures accuracy while reducing computational costs. Thus, 200 ps was selected as the uniform time scale, with multiple $\tau$ values combined into a complete simulation to ensure accuracy and reproducibility.

## S-1.4 Prediction and Discussion

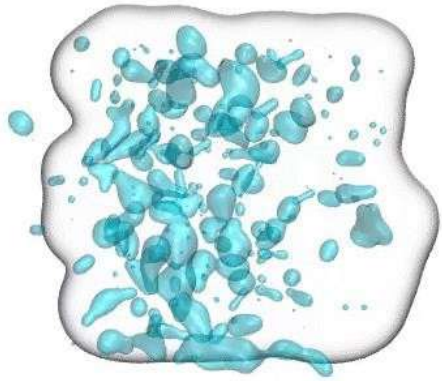

**Figure S4.** The $CO_2$ diffusion behavior in the dissolution and permeation zone of Me2F over one τ (100.2 ns-100.4 ns) window, the aggregate refers to either a single $CO_2$ molecule or a $CO_2$ cluster.

Based on simulation results, reasonable speculation and prediction can be obtained. We guess that $CO_2$ molecules tend to form clusters rather than being transported individually within the membrane during the diffusion separation process. We further verify the above hypothesis by analyzing molecular

dynamics trajectories. As shown in Figure S4, after achieving equilibrium in the simulation, we selected the trajectory of the dissolution and permeation region within the Me2F membrane from 100.2 ns to 100.4 ns to observe the motion of $CO_2$. The droplet-like structures represent $CO_2$ clusters, where smaller droplets correspond to single $CO_2$ molecule or small clusters consisting of only a few $CO_2$ molecules, while larger droplets represent clusters with relatively higher numbers of $CO_2$ molecules. The diffusion behavior of $CO_2$ in the DHP membrane is similar to that in Me2F.

**Table S4.** Comparison of Gas Permeation Properties of polymers (DHP and Me2F, in experiment, T = 35 °C, P = 1 bar; in simulation, T = 35 °C, P = concentration gradient)

| Polymer | Permeability (barrier) [2] (Experiment) | | Ideal permselectivity (Experiment) | Ideal permselectivity (Simulation) |
|---|---|---|---|---|
| | $N_2$ | $CO_2$ | $CO_2/N_2$ | $CO_2/N_2$ |
| Me2F | 370 | 5400 | 14.5 | 2.3 |
| DHP | 234 | 3400 | 14.7 | 2.6 |

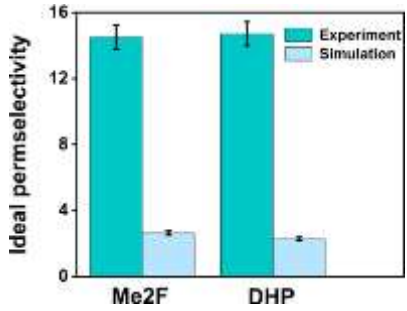


**Figure S5.** The comparison of ideal selectivity in experiment (T = 35 °C, P = 1 bar) and in simulation (T = 35 °C, P = concentration gradient).

The simulation results were compared with experimental data, as presented in Table S4 and Figure S5. A discrepancy was observed between the ideal permeability selectivity from simulations and experiments, primarily due to variations in measurement methods and experimental conditions. In experiment, gas concentration flux and separation were measured with a transmembrane pressure difference of 1 bar. Additionally, most experimental permeability ratios were

calculated using the ideal separation factor[3]. In simulation, the transmembrane pressure difference was represented by a concentration gradient, and selectivity was further decomposed into adsorption selectivity and diffusion selectivity. The diffusion coefficient quantifies the diffusion selectivity of gas molecules within the membrane along different directions, emphasizing the analysis of gas dynamics within the membrane compared to experimental methods. While some discrepancies in absolute values exist, the trends observed in the simulations are fully consistent with the experimental results This provides a more multidimensional and detailed perspective compared to experimental approaches.

Reference：


1. T. Corp, Homepage, https://zeoplusplus.org/).
2. H. W. H. Lai, F. M. Benedetti, J. M. Ahn, A. M. Robinson, Y. Wang, I. Pinnau, Z. P. Smith and Y. Xia, *Science*, 2022, **375**, 1390-1392.
3. S. Li, Z. Wan, C. Jin, J. Hao, Y. Li, X. Chen, J. Caro and A.

Huang, *Angewandte Chemie International Edition*, 2025, **64**, e202419946.